

Soft dipolar spin ice physics and the ordered phase of the frustrated $\text{Tb}_2\text{Sn}_2\text{O}_7$ pyrochlore magnet

Paul A. McClarty,¹ Pawel Stasiak,^{1,2} and Michel J. P. Gingras^{1,3}

¹*Department of Physics and Astronomy, University of Waterloo, Waterloo, ON, N2L 3G1, Canada.*

²*Department of Mathematics, University of Reading, Whiteknights, PO Box 220, Reading RG6 6AX, UK.*

³*Canadian Institute for Advanced Research, 180 Dundas Street West, Suite 1400, Toronto, ON, M5G 1Z8, Canada.*

(Dated: April 28, 2022)

From a microscopic model for the pyrochlore antiferromagnet $\text{Tb}_2\text{Sn}_2\text{O}_7$, including the crystal field Hamiltonian and interactions between the angular momenta, we compute an effective pseudospin-1/2 Hamiltonian H_{eff} that incorporates perturbatively in the effective interactions the effect of excited crystal field levels. We obtain the semiclassical ground states of H_{eff} and find a region of parameter space with a two-in/two-out spin ice configuration on each tetrahedron with ordering wavevector $\mathbf{q} = 0$ and with spins canted away from the local Ising axes as found in $\text{Tb}_2\text{Sn}_2\text{O}_7$. This ground state can also be obtained from a dipolar spin ice model in which the Ising constraint is softened. Monte Carlo simulations on the latter model reveal a region of the phase diagram with spin ice-like freezing and another with a transition into $\text{Tb}_2\text{Sn}_2\text{O}_7$ -type long range order. We comment on the differences between $\text{Tb}_2\text{Sn}_2\text{O}_7$ and the perplexing spin liquid $\text{Tb}_2\text{Ti}_2\text{O}_7$.

PACS numbers: 75.10.Dg 75.10.Jm 75.40.Cx 75.40.Gb

In recent years, much effort has been devoted to the exploration of geometrically frustrated magnetic systems [1–4]. Among the many such materials, the spin ices $\text{Ho}_2\text{Ti}_2\text{O}_7$ and $\text{Dy}_2\text{Ti}_2\text{O}_7$ [3] are remarkable for at least two reasons. Firstly, they exhibit a low temperature strongly correlated state with residual magnetic entropy and no long range order. Secondly, the mechanism leading to effectively geometrically frustrated interactions in spin ices and the equilibrium low-temperature properties that follow from them have been definitively understood [3–7]. Progress on spin ices has been made quantitatively through the dipolar spin ice model (DSIM) [3, 5] and, conceptually, via an understanding of the self-screening of the dipolar interactions [6, 7] and a description of the low-energy excitations as deconfined magnetic charges [7, 8].

That progress on spin ices has been made so steadily can be traced partly to the fact that their magnetic moments can be treated as classical and Ising-like. This is due to the fortuitous smallness of the inter-ion interactions compared to the single ion crystal field anisotropy gap. But this is also good fortune for those interested in the problem of quantum fluctuations in strongly correlated geometrically frustrated systems for, in spin ices, one can explore quantum effects by perturbing away from the Ising limit by reducing the anisotropy gap. Moreover, this is not merely an academic problem for it directly pertains to the $\text{Tb}_2\text{Sn}_2\text{O}_7$ (TSO) [9] and $\text{Tb}_2\text{Ti}_2\text{O}_7$ (TTO) [10] compounds which both exhibit rich, complex and poorly understood behaviors.

TSO has a 0.87 K transition to a long range ordered state [9, 11] where the magnetic moments obey the same (two-in/two-out) “ice rules” that hold in spin ice materials [3]. However, the ordered moments in TSO are slightly canted away from the Ising “in/out” directions while displaying fluctuations that persist down to the lowest temperature considered. TTO, in contrast, despite a Curie-Weiss temperature $\theta_{\text{CW}} \sim -14$ K set by the magnetic interactions, fails to develop long range order down to at least 50 mK [10], making it a rare example of a spin liquid in three dimensions [2]. Despite numerous experiments

aimed at exposing the essential physics at play in TSO [9, 11–14] and TTO [10, 15–17], no microscopic theory has yet been able to explain the behavior of these two materials.

Just as perturbative calculations that treat the de Broglie wavelength as a small parameter allow one to describe quantum corrections to the properties of simple liquids (e.g. argon), in the same spirit, we examine in this paper the effects of weak quantum mechanical corrections to the DSIM – a classical spin liquid of sorts [2]. As a key milestone, we consider TSO. By displaying long range order, TSO is particularly amenable to conventional experimental probes of its physics. This allows us to benchmark our calculations against known experimental results.

Starting from a microscopic model for TSO, we derive a low energy effective Hamiltonian, H_{eff} , which incorporates virtual crystal field excitations (VCFEs) about the DSIM [18]. We compute the semiclassical ground states of H_{eff} and find three phases in the vicinity of the Ising limit – one of which has the same magnetic structure as found in TSO [9]. We therefore provide a realistic microscopic explanation for the magnetic order of TSO. To explore the extent to which TSO-like order is generic among pyrochlore oxides with competing exchange, dipoles and single ion anisotropy, we consider a toy model, H_{m} , with explicit tunable single ion anisotropy. While we find that H_{m} admits a TSO-like phase over a wide range of parameters, we observe that a spin ice-like state with dynamically inhibited LRO persists close to the Ising limit. By exploring the phase diagram over the entire parameter space, we identify a fanning out of several different phases upon tuning away from the classical Heisenberg antiferromagnet spin liquid [19]. Finally, on the basis of this work, we offer a novel perspective on how TTO relates to TSO.

Effective Hamiltonian – The simplest microscopic Hamiltonian consistent with the properties of Tb^{3+} ions in TSO and with an antiferromagnetic θ_{CW} is $H = H_{\text{cf}} + V$ where H_{cf} is the crystal field Hamiltonian with parameters taken from Ref. [12]. The interaction term, $V = H_{\text{ex}} + H_{\text{dd}}$, is

the sum of the nearest neighbor isotropic exchange $H_{\text{ex}} = \mathcal{J}_{\text{ex}} \sum_{\langle i,j \rangle} \mathbf{J}_i \cdot \mathbf{J}_j$ between angular momenta \mathbf{J}_i ($J = 6$) on site i and dipole-dipole interactions $H_{\text{dd}} = \mathcal{D} r_{\text{nn}}^3 \sum_{i>j} [\mathbf{J}_i \cdot \mathbf{J}_j - 3(\mathbf{J}_i \cdot \hat{\mathbf{R}}_{ij})(\mathbf{J}_j \cdot \hat{\mathbf{R}}_{ij})] |\mathbf{R}_{ij}|^{-3}$. The dipole coupling $\mathcal{D} = \mu_0 (g\mu_B)^2 / 4\pi r_{\text{nn}}^3 = 0.029$ K where the Landé factor of Tb^{3+} is $g = 3/2$ and the exchange has been estimated to be $\mathcal{J}_{\text{ex}} \sim 0.08$ K [12]. $\mathbf{R}_{ij} = \mathbf{R}_i - \mathbf{R}_j$ where \mathbf{R}_i is the position of the magnetic ion on site i . The nearest neighbor distance $r_{\text{nn}} = 3.69\text{\AA} = a\sqrt{2}/4$ [9] and a is the edge length of the cubic unit cell. Throughout this paper, the long range dipolar interactions are handled via the Ewald method [20].

Diagonalizing H_{cf} gives a spectrum of $2J + 1 = 13$ states with an Ising-like ground state doublet separated from the first excited doublet by a gap $\Delta \sim 13.8$ K [12]. Because the interactions, V , are much smaller than Δ , we treat V as a perturbation. Using degenerate perturbation theory, we derive an effective Hamiltonian, H_{eff} , acting in the space \mathfrak{M} spanned by the ground doublet on each site and which includes, to leading order in V^2/Δ , the effect of admixing of the excited crystal field levels into the low energy space (i.e. VCFEs) [18]. Because the low energy space is two-dimensional on each site, H_{eff} can be rendered in the form of a pseudospin-1/2 (\mathcal{S}_{eff}) Hamiltonian [18]. In the limit $V/\Delta \rightarrow 0$, $H_{\text{eff}} \sim O(V)$ is the projection of V onto the ground doublet which gives the dipolar spin ice Ising model (DSIM) [5, 18, 21]. Terms to order V^2/Δ deform H_{eff} away from the Ising limit.

H_{eff} ground states – To examine the effects of excited crystal field levels on the spin correlations, we determine the semiclassical ground states of H_{eff} on a cubic unit cell with periodic boundary conditions by replacing the pseudospins, $\mathcal{S}_{\text{eff}}(\mathbf{R}_i)$, by classical spins of fixed length $1/2$. This is akin to finding a semiclassical Néel ordered phase as the leading description of the broken symmetry phase in a quantum Heisenberg antiferromagnet. The ground state phase diagram as the anisotropy gap Δ and $\mathcal{D}/\mathcal{J}_{\text{ex}}$ are varied is shown in panel (a) of Fig. 1. For $\Delta = 13.8$ K corresponding to TSO, the ground state for weakly antiferromagnetic exchange $\mathcal{J}_{\text{ex}} < 0.050$ K ($\mathcal{D}/\mathcal{J}_{\text{ex}} > 0.58$) has a $\mathbf{q} = 001$ ordering wavevector with zero bulk magnetization and the two-in/two-out spin ice rule satisfied by the local [111] (Ising) components of \mathcal{S}_{eff} on each tetrahedron. Three body interactions in H_{eff} cause the $\mathcal{S}_{\text{eff}}(\mathbf{R}_i)$ to cant away from the local Ising directions. The “uncanted” variant of this $\mathbf{q} = 001$ long range ordered spin ice (LRSI₀₀₁) state is one of the two ground states of the DSIM for $1/\Delta = 0$ [5] (see Fig. 1). For $\mathcal{J}_{\text{ex}} > 0.050$ K ($\mathcal{D}/\mathcal{J}_{\text{ex}} < 0.58$) and $\Delta = 13.8$ K, instead of the all-in/all-out state observed in the DSIM [5] (which appears here only for $1/\Delta \lesssim 0.04$ K⁻¹), we find that the ground state is an ordered ice state with ordering wavevector $\mathbf{q} = 0$ and with the ice rule satisfied on each tetrahedron (LRSI₀₀₀). Quantum fluctuations away from these classical ground states are currently being investigated and will be reported elsewhere. The all-in/all-out to LRSI₀₀₀ phase boundary, computed for fixed \mathcal{D} , has a maximum for small $\mathcal{D}/\mathcal{J}_{\text{ex}}$ which indicates that terms to order V^2/Δ in perturbation theory are not adequate to ac-

count for the phase boundary for too small Δ .

The ground states spin configurations determined from H_{eff} are the semiclassical expectation values of the pseudospins, \mathcal{S}_{eff} . However, the physical observables are, rather, the expectation values of the angular momenta $\langle J^{\tilde{\alpha}} \rangle$ for $\tilde{\alpha} = \tilde{x}, \tilde{y}, \tilde{z}$. We therefore compute the $\langle J^{\tilde{\alpha}} \rangle$ from the $\mathcal{S}_{\text{eff}}^{\tilde{\alpha}}$ expectation values. We do this perturbatively in the interactions V finding

$$\langle J^{\tilde{\alpha}} \rangle = \langle \mathcal{P} J^{\tilde{\alpha}} \mathcal{P} \rangle + \langle \mathcal{P} V Q J^{\tilde{\alpha}} \mathcal{P} \rangle + \langle \mathcal{P} J^{\tilde{\alpha}} Q V \mathcal{P} \rangle + \dots \quad (1)$$

for the expectation values of $\langle J^{\tilde{\alpha}} \rangle$ within the low energy subspace where $Q = \sum_{|\psi\rangle \in \mathfrak{M}} |\psi\rangle \langle \psi| / (E_g - E_{|\psi\rangle})$ and E_g is the ground state energy of the unperturbed ground crystal field doublet. The tilde over the components of $\langle J^{\tilde{\alpha}} \rangle$ indicates that the components are taken in the local $\tilde{x} - \tilde{y} - \tilde{z}$ frame on each sublattice [20]. The expansion in operators on the right hand side of Eq. (1) can be rendered in the form of pseudospin-1/2 operators with coefficients that are computed numerically.

We are mainly interested in the $\mathbf{q} = 0$ ordered ice state (LRSI₀₀₀). We compute H_{eff} on a cubic unit cell and consider a state vector, within the pseudospin \mathfrak{M} space, corresponding to the LRSI₀₀₀ with canted $\mathcal{S}_{\text{eff}}(\mathbf{R}_i)$ that minimizes the classical energy. The state vector corresponding to such semiclassical ground state is a direct product of canted pseudospins-1/2 states on each site of the cubic cell. The expectation value of $J^{\tilde{z}}$, $\langle J^{\tilde{z}} \rangle$, is computed from Eq. (1) on each of the 16 sites as a function of \mathcal{J}_{ex} . As one would expect from Eq. (1) the magnitude of $\langle J^{\tilde{z}} \rangle$ changes as \mathcal{J}_{ex} varies. However, the relative signs of $J^{\tilde{z}}$ on each of the sites are *preserved*, so the identification of the $\mathbf{q} = 0$ ordered spin ice state is *unaltered* by the operator correction of Eq. (1). Next, we find the $\langle J^{\tilde{x}} \rangle$ and $\langle J^{\tilde{y}} \rangle$ expectation values on each lattice site for which the only contributions come from the terms linear in V in Eq. (1). The result of this calculation is that the $\langle J^{\tilde{\alpha}} \rangle$ ground state configuration is the same magnetic structure of canted magnetic moments as observed in TSO [9] – a structure that we henceforth refer to as LRSI_{TSO}. Note that it is crucial that the ordered moments be described via the observables $\langle J^{\tilde{\alpha}} \rangle$ in Eq. (1), as sole consideration of the expectation values of the $\mathcal{S}_{\text{eff}}(\mathbf{R}_i)$ does not even give qualitatively the correct canting direction and disagrees with the canting experimentally observed in TSO [9].

Soft dipolar spin ice model – The essential physics of H_{eff} is that VCFEs lead to (i) a softening of the otherwise Ising spins and (ii) a new (LRSI₀₀₀) ordered spin ice state not present in the DSIM [5]. To explore the effects of the softened Ising constraint and the extent to which the appearance of a LRSI₀₀₀ state is generic in dipolar pyrochlore systems with softened [111] Ising anisotropy, we investigate a toy model, H_{m} , with an explicitly anisotropic g -tensor.

We take $H_{\text{m}} \equiv H_{\text{ex}} + H_{\text{dd}}$ as used in the microscopic model H discussed above where the \mathbf{J}_i are taken to be Heisenberg spins. For this model, we denote the exchange and dipole couplings by J and D respectively. We incorporate the anisotropy by introducing spins-1/2 \mathcal{S} with components defined via $(J^{\tilde{x}}, J^{\tilde{y}}, J^{\tilde{z}}) \rightarrow (g_{\perp} S^{\tilde{x}}, g_{\perp} S^{\tilde{y}}, g_{\parallel} S^{\tilde{z}})$ with $g_{\parallel} > g_{\perp}$ to achieve an Ising-like anisotropy. Whereas, in H_{eff} , the spin softness is generated through VCFEs, in H_{m} we include

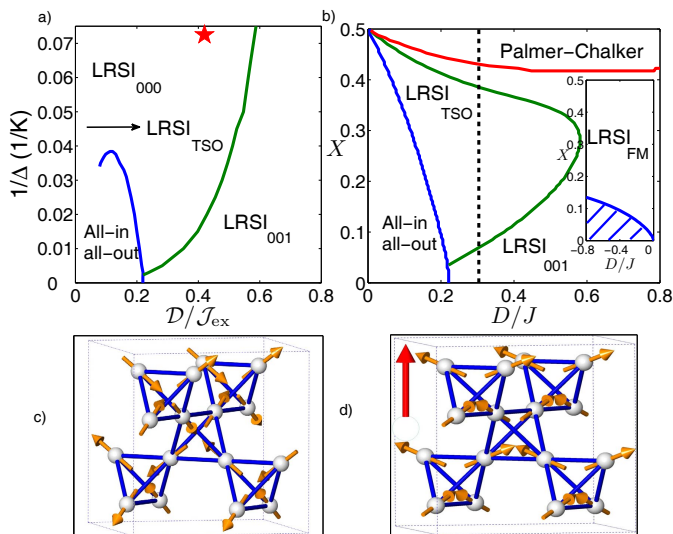


FIG. 1: (color online). (a) Semiclassical ground state of H_{eff} on a single cubic unit cell as a function of $1/\Delta$ and J_{ex}/D . The star indicates the estimated microscopic parameters of TSO. (b) Ground states of the classical spin model H_{m} as a function of couplings D/J and the anisotropy X . Ground states are shown for antiferromagnetic J and an Ising anisotropy. Note the similar topology of the phase diagrams in (a) and (b) close to $D/J, D/J_{\text{ex}} \approx 0.2$ and small anisotropy (small $1/\Delta, X$). The inset shows the ground states for ferromagnetic J for $0 < X < 1$. The vertical dashed line indicates the line along which Monte Carlo simulations have been carried out. The lower panels show the LRSI_{TSO} (c) and LRSI₀₀₁ (d) spin configurations on a single cubic unit cell. The vertical (red) arrow in (d) shows the $[0, 0, 1]$ direction of the bulk net moment.

the effects of this physics at the outset. We parameterize the anisotropy $\mathbf{g} \equiv (g_{\perp}, g_{\perp}, g_{\parallel})$ by the parameter X such that $\mathbf{g} = \eta(X, X, 1 - X)$ with η chosen so that \mathbf{g} is a unit vector. When $X = 0$, (i.e. $g_{\perp} = 0$), we obtain a model that couples only the Ising components of the \mathbf{S} vectors. This model for $J = 0$ was studied in Ref. [22] and a related model with $D = 0, X = 1/2$ and ferromagnetic J , but with a single ion anisotropy $-\Gamma(S_i^z)^2$, has been investigated [23].

Panel (b) of Figure 1 displays the semiclassical ground states of H_{m} as X and D/J are varied. The ground states are computed on a single cubic unit cell using zero temperature Monte Carlo. The main figure shows the ground states for $0 \leq X < 0.5$ (Ising anisotropy) and antiferromagnetic $J > 0$. The point ($D/J = 0, X = 0.5$) corresponds to the classical Heisenberg antiferromagnet spin liquid on the pyrochlore lattice [19], from which four long range ordered phases fan out. For small D/J , the ground state is an all-in/all-out (AIAO) state with ordering wavevector $\mathbf{q} = 0$ with no canting of the spins away from the Ising directions. For large D/J , one finds LRSI₀₀₁ states with ordering wavevector $\mathbf{q} = 001$ with the ice rule satisfied on each tetrahedron. The AIAO state and the LRSI₀₀₁ state are both ground states of the DSIM and the boundary between them for $X = 0$ is consistent with earlier findings [5]. We find that the canting angle away from the

Ising directions varies smoothly away from 0 (for $X = 0$) in the LRSI₀₀₁ state as the parameters vary. In the isotropic ($X = 1/2$, Heisenberg) limit, we recover the Palmer-Chalker ground state [24]. We find that this state remains the ground state even away from the isotropic limit with spins lying in the local $\tilde{x}\tilde{y}$ planes. At the center of the figure is a dome in which the ground state is a LRSI_{TSO} state with D/J and X dependent canting angles. The inset shows the ground states for ferromagnetic exchange ($J < 0$). The LRSI₀₀₁ ground state (for $X = 0$) extends to finite X (dashed region), whereupon it gives way to a $\mathbf{q} = 0$ two-in/two-out ordered state that we label LRSI_{FM}. The distinction between LRSI_{TSO} and LRSI_{FM} is that, in the former (latter), the net moment on each tetrahedron is smaller (larger) than the moment $4\mu/\sqrt{3}$ of a $\mathbf{q} = 0$ two-in/two-out state with moments μ constrained to lie along the $\langle 111 \rangle$ Ising directions. The labelling of the regions in the figure is independent of the canting angle away from the $\langle 111 \rangle$ directions. The canting angle (not indicated) increases as X increases with discontinuities at the phase boundaries. Within the LRSI_{TSO} phase, the general trend in the canting angle is for it to decrease as D/J increases.

We have explored the finite temperature phase diagram along the line $D/J = 0.3$ using Monte Carlo (MC) simulations with parallel tempering. We chose this line because it cuts through three sets of ground states as X is varied (see panel (b) of Fig. 1). For Ising interactions, $X = 0$, upon lowering the temperature, the conventional paramagnet freezes into a spin ice state characterized by a two-in/two-out constraint on each tetrahedron but without conventional LRO. While one would expect some residual entropy, in this case, it does not coincide with the Pauling entropy of spin ice because the spins are classical 3-component spins with a magnetic specific heat per spin of k_B at $T = 0$ (see lower right panel of Fig. 2). Of particular interest, this freezing is observed at finite X up to the boundary between LRSI₀₀₁ and LRSI_{TSO}. The freezing temperatures are indicated in the top panel of Fig. 2 for $X \lesssim 0.07$. For $X \gtrsim 0.07$ and $D/J = 0.3$, the simulations equilibrate easily with strong evidence of phase transitions into long-range ordered phases corresponding to the ground states of Fig. 1. The transition temperatures from the heat capacity peak are plotted in the top panel of Fig. 2. The lower panels of Fig. 2 shows for $X = 0.25$, within the LRSI_{TSO} dome, the order parameter $Y_{\mathbf{q}=0}$ (an order parameter for the $\mathbf{q} = 0$ ordered ice [25]) and the specific heat for different system sizes measured in L – the length of the cubic simulation cell in units of the cubic unit cell edge. Since the simulations reveal a freezing transition for $X \lesssim 0.07$ and LRO at finite temperature in the (reentrant) LRSI₀₀₁ region around $X = 0.4$ (see top panel of Fig. 2), there exists a crossover between a freezing transition ($X \lesssim X^*$) and a phase transition to LRO ($X \gtrsim X^*$) within the LRSI₀₀₁ region of Fig. 1b. We have run a series of simulations for $L = 2, 3$ and 4 finding that this boundary lies near $X^* \approx 0.35$, largely independently of D/J as far as we can tell. We always observe the onset of finite temperature LRO within the LRSI_{TSO} dome in Fig. 1b.

Materials context – Given the considerable microscopic

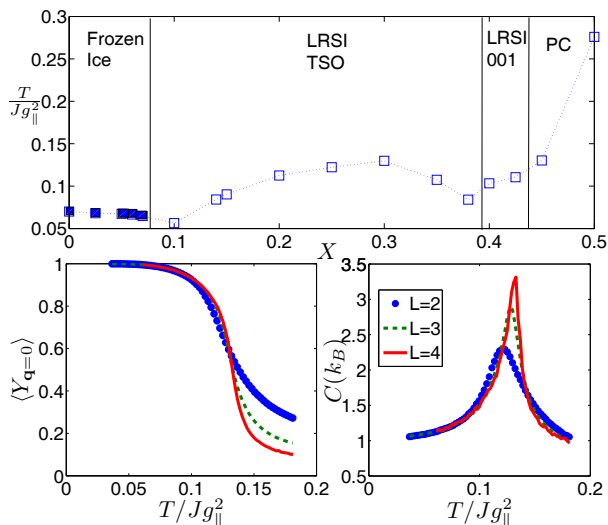


FIG. 2: (color online). Selected Monte Carlo simulation results on H_m . Simulations have been carried out along the line $D/J = 0.3$. The upper panel shows the freezing temperatures (for $X < 0.07$) and transition temperatures ($X > 0.07$) determined from the heat capacity peak for system size $L = 3$. The ground states as a function of X are indicated. The lower left hand panel shows, for $X = 0.25$, the increase of the $\mathbf{q} = 0$ ordered ice order parameter $Y_{\mathbf{q}=0}$ at the temperature is lowered for $L = 2, 3, 4$. The lower right hand panel shows the heat capacity for $X = 0.25$ and $L = 2, 3, 4$.

similarities between TSO and TTO, one wonders whether H_m might help shed some light on the low temperature collective paramagnetism of TTO. Since the anisotropy gap in TTO is larger than in TSO, one might consider TTO to have the larger Ising anisotropy (smaller X) and to lie in the frozen canted spin ice regime of H_m . Interestingly, TTO does exhibit hysteresis and a frequency dependent a.c. susceptibility [16, 17] below about 350 mK which is consistent with a slowing down of the dynamics. However, this glassiness has been suggested to come from only a fraction of the moments [16], the rest exhibiting fast spin dynamics down to the lowest observed temperatures consistent with the lack of LRO [10]. On the other hand, low temperature ($T \lesssim 500$ mK) spin dynamics does not distinguish the two materials for they are also observed in TSO in spite of the LRO [13]. More critically, we note that the mechanism underlying the persistent spin dynamics in these materials as in other pyrochlores with LRO and gapped collective excitations (e.g. $\text{Gd}_2\text{Sn}_2\text{O}_7$ [26]) remains an important open problem [4, 26]. Since H_m captures the LRO in TSO which remains dynamical, we cannot rule out the possibility that dynamics may also occur in TTO at $T \lesssim 350$ mK alongside spin ice-like freezing as we find in H_m . Further investigations will be necessary to settle this matter.

Conclusion – We have shown that a low energy effective Hamiltonian H_{eff} for $\text{Tb}_2\text{Sn}_2\text{O}_7$ derived from a microscopic model including crystal field, antiferromagnetic exchange and dipolar interactions exhibits semiclassical ground states coinciding with the magnetic structure of $\text{Tb}_2\text{Sn}_2\text{O}_7$ (LRSI_{TSO}

states) [9]. We used this result to motivate the study of a classical spin model H_m referred to as a soft dipolar spin ice model (SDSIM). This model also exhibits a finite temperature transition into LRSI_{TSO} states over a large portion of its phase diagram indicating that it captures the essential physics obtained from the microscopic model. Therefore, we are confident that we have correctly identified the predominant physics leading to the $\mathbf{q} = 0$ spin ice ordered phase of $\text{Tb}_2\text{Sn}_2\text{O}_7$ and the concurrent spin canting away from the Ising directions. A corollary of our results is that spin-lattice couplings are not necessary to account for the long range ordered phase of $\text{Tb}_2\text{Sn}_2\text{O}_7$. More generally, the SDSIM reveals the competing and important effects of single ion anisotropy, exchange and dipolar interactions in rare earth pyrochlore oxides. We hope that our toy model H_m will serve as a bridge between these materials and ultimately help to unravel the fascinating phenomena at play in the $\text{Tb}_2\text{Ti}_2\text{O}_7$ spin liquid material.

We thank B. Gaulin, P. Holdsworth and J. Ruff for useful discussions. This research was funded by the NSERC of Canada and the Canada Research Chair program (M. G., Tier I). We acknowledge the use of computational resources from SHARCNET.

-
- [1] H.T. Diep, *Frustrated Spin Systems*, (World Scientific Publishing Co. Pte. Ltd., 2004, Hackensack).
 - [2] L. Balents, *Nature* **464**, 199 (2010).
 - [3] S. T. Bramwell and M. J. P. Gingras, *Science* **294**, 1495 (2001).
 - [4] J. S. Gardner, M. J. P. Gingras and J. E. Greedan, *Rev. Mod. Phys.* **82**, 53 (2010).
 - [5] R. G. Melko and M. J. P. Gingras, *J. Phys.: Condens. Matter* **16**, R1277 (2004) and references therein.
 - [6] M. J. P. Gingras and B. C. den Hertog, *Can. J. Phys.* **79**, 1339 (2001); S. V. Isakov, R. Moessner and S. L. Sondhi, *Phys. Rev. Lett.* **95**, 217201 (2005).
 - [7] C. Castelnovo, R. Moessner and S. L. Sondhi, *Nature* **451**, 42 (2008).
 - [8] L. D. C. Jaubert and P. C. W. Holdsworth, *Nature Physics* **5**, 258 (2009).
 - [9] I. Mirebeau *et al.*, *Phys. Rev. Lett.* **94**, 246402 (2005).
 - [10] J. S. Gardner *et al.*, *Phys. Rev. Lett.* **82**, 1012 (1999);
 - [11] K. Matsuhira *et al.*, *J. Phys. Soc. Jpn.* **71**, 1576 (2002).
 - [12] I. Mirebeau, P. Bonville and M. Hennion, *Phys. Rev. B* **76**, 184436 (2007).
 - [13] P. Dalmas de Réotier *et al.*, *Phys. Rev. Lett.* **96**, 127202 (2006); F. Bert *et al.*, *Phys. Rev. Lett.* **97**, 117203 (2006); Y. Chapis *et al.*, *J. Phys.: Condens. Matter* **19**, 446206 (2007); S. R. Giblin *et al.*, *Phys. Rev. Lett.* **101**, 237201 (2008); K. Rule *et al.*, *Phys. Rev. B* **76**, 212405 (2007); I. Mirebeau *et al.*, *Phys. Rev. B* **78**, 174416 (2008); K. Rule *et al.*, *J. Phys.: Condens. Matter* **21**, 486005 (2009).
 - [14] I. Mirebeau *et al.*, *Phys. Rev. B* **80**, 220407(R) (2009); *ibid.*, *High Pressure Physics* **30**, 3 (2010).
 - [15] J. S. Gardner *et al.*, *Phys. Rev. B* **64**, 224416 (2001); Y. Yasui *et al.*, *J. Phys. Soc. Jpn.* **71**, 599 (2002).
 - [16] J. S. Gardner *et al.*, *Phys. Rev. B* **68**, 180401(R) (2003).
 - [17] N. Hamaguchi *et al.*, *Phys. Rev. B* **69**, 132413 (2004).
 - [18] H. R. Molavian, M. J. P. Gingras and B. Canals, *Phys. Rev. Lett.*

- 98, 157204 (2007).
- [19] R. Moessner and J. T. Chalker, Phys. Rev. Lett. **58**, 12049 (1998).
- [20] M. Enjalran and M. J. P. Gingras, Phys. Rev. B **70**, 174426 (2004). Y.-J. Kao *et al.*, Phys. Rev. B **68**, 172407 (2003).
- [21] M. J. P. Gingras, arXiv:0903.2772.
- [22] S. L. Chamberlain, S. T. Hess and L. R. Corruccini Phys. Lett. A **323**, 310 (2004).
- [23] J. D. M. Champion *et al.*, Europhys. Lett. **57**, 93 (2002). Adding long range dipolar interactions to Champion *et al.*'s model also gives a spin canting similar to that of TSO. However, H_m , considered in this paper, is closer conceptually to the formally derived effective microscopic model H_{eff} .
- [24] S. E. Palmer and J. T. Chalker, Phys. Rev. B **62**, 488 (2000).
- [25] This order parameter is defined as follows: we introduce vectors I_u^α with components $I_1 = (1, 1, -1, -1)$, $I_2 = (1, -1, -1, 1)$ and $I_3 = (-1, 1, 1, -1)$. These are the three ways in which Ising components of spins in spin ice can be arranged on a single tetrahedron. Note that $\mathbf{I}_u \cdot \mathbf{I}_v = 4\delta_{uv}$. The order parameter $Y_{\mathbf{q}=0}$ is $(1/N) |\sum_u \sum_{i,a} \sigma_i^a I_u^a|$ where $\sigma_i^a = \pm 1$ is the sign of the Ising component of the spin on sublattice a , fcc vector i and N is the number of spins. $\langle Y_{\mathbf{q}=0} \rangle$ denotes the thermally averaged order parameter.
- [26] P. A. McClarty *et al.*, arXiv:1011.5689.